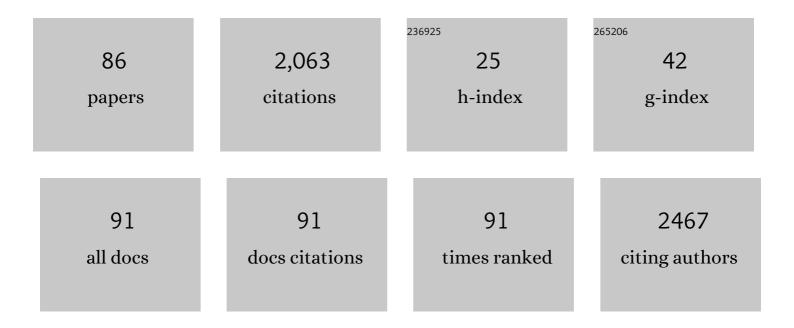
List of Publications by Year in descending order

Source: https://exaly.com/author-pdf/8673900/publications.pdf Version: 2024-02-01



MICHELA FRATINI

#	Article	IF	CITATIONS
1	Scale-free structural organization of oxygen interstitials in La2CuO4+y. Nature, 2010, 466, 841-844.	27.8	236
2	Evolution and control of oxygen order in a cuprateÂsuperconductor. Nature Materials, 2011, 10, 733-736.	27.5	148
3	SYRMEP Tomo Project: a graphical user interface for customizing CT reconstruction workflows. Advanced Structural and Chemical Imaging, 2017, 3, 4.	4.0	111
4	Optimum inhomogeneity of local lattice distortions in La ₂ CuO _{4+ <i>y</i>} . Proceedings of the National Academy of Sciences of the United States of America, 2012, 109, 15685-15690.	7.1	109
5	Feshbach resonance and mesoscopic phase separation near a quantum critical point in multiband FeAs-based superconductors. Superconductor Science and Technology, 2009, 22, 014004.	3.5	77
6	Simultaneous submicrometric 3D imaging of the micro-vascular network and the neuronal system in a mouse spinal cord. Scientific Reports, 2015, 5, 8514.	3.3	73
7	The effect of internal pressure on the tetragonal to monoclinic structural phase transition in ReOFeAs: the case of NdOFeAs. Superconductor Science and Technology, 2008, 21, 092002.	3.5	70
8	Generic acquisition protocol for quantitative MRI of the spinal cord. Nature Protocols, 2021, 16, 4611-4632.	12.0	65
9	X-Ray Phase Contrast Tomography Reveals Early Vascular Alterations and Neuronal Loss in a Multiple Sclerosis Model. Scientific Reports, 2017, 7, 5890.	3.3	64
10	Exploring Alzheimer's disease mouse brain through X-ray phase contrast tomography: From the cell to the organ. NeuroImage, 2019, 184, 490-495.	4.2	56
11	in the high-temperature superconductor Bi <mmi:math xmlns:mml="http://www.w3.org/1998/Math/MathML" display="inline"><mml:msub><mml:mrow /><mml:mn>2</mml:mn></mml:mrow </mml:msub>Sr<mml:math xmlns:mml="http://www.w3.org/1998/Math/MathML" display="inline"><mml:msub><mml:mrow< td=""><td>3.2</td><td>45</td></mml:mrow<></mml:msub></mml:math </mmi:math 	3.2	45
12	Intrinsic Patterns of Coupling between Correlation and Amplitude of Low-Frequency fMRI Fluctuations Are Disrupted in Degenerative Dementia Mainly due to Functional Disconnection. PLoS ONE, 2015, 10, e0120988.	2.5	43
13	Brain Networks Underlying Eye's Pupil Dynamics. Frontiers in Neuroscience, 2019, 13, 965.	2.8	42
14	Quantitative 3D investigation of Neuronal network in mouse spinal cord model. Scientific Reports, 2017, 7, 41054.	3.3	40
15	The Feshbach resonance and nanoscale phase separation in a polaron liquid near the quantum critical point for a polaron Wigner crystal. Journal of Physics: Conference Series, 2008, 108, 012036.	0.4	35
16	A Model for Liquid-Striped Liquid Phase Separation in Liquids ofÂAnisotropic Polarons. Journal of Superconductivity and Novel Magnetism, 2009, 22, 529-533.	1.8	33
17	Quantitative Chemical Imaging of the Intracellular Spatial Distribution of Fundamental Elements and Light Metals in Single Cells. Analytical Chemistry, 2014, 86, 5108-5115.	6.5	32
18	Nanoscale quantification of intracellular element concentration by X-ray fluorescence microscopy combined with X-ray phase contrast nanotomography. Applied Physics Letters, 2018, 112, .	3.3	32

#	Article	IF	CITATIONS
19	Heterogeneous and self-organizing mineralization of bone matrix promoted by hydroxyapatite nanoparticles. Nanoscale, 2017, 9, 17274-17283.	5.6	31
20	Local structure of ReFeAsO (Re=La, Pr, Nd, Sm) oxypnictides studied by Fe K-edge EXAFS. Europhysics Letters, 2009, 87, 26005.	2.0	30
21	Imaging collagen packing dynamics during mineralization of engineered bone tissue. Acta Biomaterialia, 2015, 23, 309-316.	8.3	30
22	Three dimensional visualization of engineered bone and soft tissue by combined x-ray micro-diffraction and phase contrast tomography. Physics in Medicine and Biology, 2014, 59, 189-201.	3.0	27
23	Virtual unrolling and deciphering of Herculaneum papyri by X-ray phase-contrast tomography. Scientific Reports, 2016, 6, 27227.	3.3	27
24	Xâ€ray microtomography and phylogenomics provide insights into the morphology and evolution of an enigmatic Mesozoic insect larva. Systematic Entomology, 2021, 46, 672-684.	3.9	27
25	The Microstrain-Doping Phase Diagram of the Iron Pnictides: Heterostructures at Atomic Limit. Journal of Superconductivity and Novel Magnetism, 2009, 22, 589-593. Isotope effect on the <mml:math <="" td="" xmlns:mml="http://www.w3.org/1998/Math/MathML"><td>1.8</td><td>26</td></mml:math>	1.8	26
26	display="inline"> < mml:mrow> < mml:msub> < mml:mtext> E < /mml:mtext> < mml:mrow> < mml:mn> 2 < /mml:mn> < m and mesoscopic phase separation near the electronic topological transition in < mml:math xmlns:mml="http://www.w3.org/1998/Math/MathML" display="inline"> < mml:mrow> < mml:msub> < mml:mrow> < mml:mtext> Mg < /mml:mtext> < /mml:mrow> < mml:mrow	3.2	25
27	Physical Review B, 2009, 80, . Where is it and how much? Mapping and quantifying elements in single cells. Analyst, The, 2016, 141, 5221-5235.	3.5	23
28	RE L ₃ x-ray absorption study of REO _{1â^'<i>x</i>} F _{<i>x</i>} FeAs (RE =) Tj ET	Qq0 ₈ 00rş	gBT /Overlock
29	Multiscale pink-beam microCT imaging at the ESRF-ID17 biomedical beamline. Journal of Synchrotron Radiation, 2020, 27, 1347-1357.	2.4	21
30	The Misfit Strain Critical Point in the 3D Phase Diagrams ofÂCuprates. Journal of Superconductivity and Novel Magnetism, 2009, 22, 299-303.	1.8	20
31	Intracellular concentration map of magnesium in whole cells by combined use of X-ray fluorescence microscopy and atomic force microscopy. Spectrochimica Acta, Part B: Atomic Spectroscopy, 2011, 66, 834-840.	2.9	20
32	Size evolution of the oxygen interstitial nanowires in La2CuO4+yby thermal treatments and x-ray continuous illumination. Superconductor Science and Technology, 2012, 25, 124004.	3.5	20
33	On the impact of physiological noise in spinal cord functional MRI. Journal of Magnetic Resonance Imaging, 2014, 40, 770-777.	3.4	20
34	The Tetragonal to Orthorhombic Structural Phase Transition inÂMultiband FeAs-based Superconductors. Journal of Superconductivity and Novel Magnetism, 2009, 22, 305-308.	1.8	19
35	xmins:mml= http://www.w3.org/1998/Math/Math/Math/MathML_display= inline > <mml:msub><mml:mrow /><mml:mrow><mml:mn>1</mml:mn><mml:mo>â²</mml:mo> <mml:mi>x</mml:mi></mml:mrow>xmlns:mml="http://www.w3.org/1998/Math/MathML" display="inline"><mml:mi>x</mml:mi></mml:mrow /><mml:mi>x</mml:mi></mml:msub> AsO <mml:mth="inline"><mml:msub></mml:msub>AsO<td>>3.2</td><td>ath>Ru<mml 19</mml </td></mml:mth="inline">	>3.2	ath>Ru <mml 19</mml
36	Assessment of plaque morphology in Alzheimer's mouse cerebellum using three-dimensional X-ray phase-based virtual histology. Scientific Reports, 2020, 10, 11233.	3.3	19

#	Article	IF	CITATIONS
37	Single cell versus large population analysis: cell variability in elemental intracellular concentration and distribution. Analytical and Bioanalytical Chemistry, 2018, 410, 337-348.	3.7	17
38	X-ray phase contrast microscopy at 300 nm resolution with laboratory sources. Optics Express, 2010, 18, 15998.	3.4	16
39	Controlling Photoinduced Electron Transfer Via Defects Self-Organization for Novel Functional Macromolecular Systems. Current Protein and Peptide Science, 2014, 15, 394-399.	1.4	15
40	Characterization of mouse spinal cord vascular network by means of synchrotron radiation X-ray phase contrast tomography. Physica Medica, 2016, 32, 1779-1784.	0.7	15
41	Task-Related Modulations of BOLD Low-Frequency Fluctuations within the Default Mode Network. Frontiers in Physics, 2017, 5, .	2.1	15
42	An improved ring removal procedure for in-line x-ray phase contrast tomography. Physics in Medicine and Biology, 2018, 63, 045007.	3.0	14
43	Evaluation of denoising strategies for taskâ€based functional connectivity: Equalizing residual motion artifacts between rest and cognitively demanding tasks. Human Brain Mapping, 2021, 42, 1805-1828.	3.6	14
44	Scale-invariant rearrangement of resting state networks in the human brain under sustained stimulation. NeuroImage, 2018, 179, 570-581.	4.2	13
45	Imaging regenerating bone tissue based on neural networks applied to micro-diffraction measurements. Applied Physics Letters, 2013, 103, 253703.	3.3	12
46	X-ray fluorescence microscopy of light elements in cells: self-absorption correction by integration of compositional and morphological measurements. Journal of Physics: Conference Series, 2013, 463, 012022.	0.4	12
47	X-ray Phase Contrast Tomography Serves Preclinical Investigation of Neurodegenerative Diseases. Frontiers in Neuroscience, 2020, 14, 584161.	2.8	12
48	Controlling the Critical Temperature in Mg1â^'x Al x B2. Journal of Superconductivity and Novel Magnetism, 2007, 20, 495-501.	1.8	11
49	X-Rays Writing/Reading of Charge Density Waves in the CuO2 Plane of a Simple Cuprate Superconductor. Condensed Matter, 2017, 2, 26.	1.8	11
50	X-ray phase contrast tomography for the investigation of amyotrophic lateral sclerosis. Journal of Synchrotron Radiation, 2020, 27, 1042-1048.	2.4	11
51	Control of silver–polymer aggregation mechanism by primary particle spatial correlations in dynamic fractal-like geometry. Nanoscale, 2011, 3, 3774.	5.6	10
52	High-Resolution X-Ray Techniques as New Tool to Investigate the 3D Vascularization of Engineered-Bone Tissue. Frontiers in Bioengineering and Biotechnology, 2015, 3, 133.	4.1	10
53	Controlling mesoscopic phase separation near electronic topological transitions via quenched disorder in ternary diborides. Journal of Physics Condensed Matter, 2008, 20, 434222.	1.8	9
54	Fractal Dimension Analysis of High-Resolution X-Ray Phase Contrast Micro-Tomography Images at Different Threshold Levels in a Mouse Spinal Cord. Condensed Matter, 2018, 3, 48.	1.8	9

#	Article	IF	CITATIONS
55	Angular distribution of field emitted electrons from vertically aligned carbon nanotube arrays. Applied Physics Letters, 2012, 100, .	3.3	8
56	Assessment of the effects of different sample perfusion procedures on phase-contrast tomographic images of mouse spinal cord. Journal of Instrumentation, 2018, 13, C03027-C03027.	1.2	7
57	Multiscale Imaging Approach for Studying the Central Nervous System: Methodology and Perspective. Frontiers in Neuroscience, 2020, 14, 72.	2.8	7
58	Flux Dynamics in NdO1â^'x F x FeAs Bulk Sample. Journal of Superconductivity and Novel Magnetism, 2009, 22, 549-552.	1.8	6
59	Assessing denoising strategies to increase signal to noise ratio in spinal cord and in brain cortical and subcortical regions. Journal of Instrumentation, 2018, 13, C02028-C02028.	1.2	6
60	Brain Network Modularity During a Sustained Working-Memory Task. Frontiers in Physiology, 2020, 11, 422.	2.8	6
61	Investigation of the human pineal gland 3D organization by X-ray phase contrast tomography. Journal of Structural Biology, 2020, 212, 107659.	2.8	5
62	3D Spatial Distribution of Nanoparticles in Mice Brain Metastases by X-ray Phase-Contrast Tomography. Frontiers in Oncology, 2021, 11, 554668.	2.8	5
63	Steerable3D: An ImageJ plugin for neurovascular enhancement in 3-D segmentation. Physica Medica, 2021, 81, 197-209.	0.7	5
64	High resolution 3D visualization of the spinal cord in a post-mortem murine model. Biomedical Optics Express, 2020, 11, 2235.	2.9	5
65	Activation Energy of the Photo Induced Q2 Oxygen Ordered Phase in the La2CuO4.08 Superconductor. Journal of Superconductivity and Novel Magnetism, 2005, 18, 671-674.	0.5	4
66	Anomalous Thermal Expansion in Superconducting Mg1â^' x Al x B2 System. Journal of Superconductivity and Novel Magnetism, 2005, 18, 737-741.	0.5	4
67	Manipulation of Mesoscopic Phase Separation byÂX-rayÂlllumination. Journal of Superconductivity and Novel Magnetism, 2007, 20, 551-554.	1.8	3
68	X-ray micro-beam techniques and phase contrast tomography applied to biomaterials. Nuclear Instruments & Methods in Physics Research B, 2015, 364, 93-97.	1.4	3
69	Carbon nanotube—Based cold cathodes: Field emission angular properties and temporal stability. Journal of Applied Physics, 2016, 120, 164305.	2.5	3
70	Assessment and Imaging of Intracellular Magnesium in SaOS-2 Osteosarcoma Cells and Its Role in Proliferation. Nutrients, 2021, 13, 1376.	4.1	3
71	T c as a Function of Electron Doping in Mg10B2 Using Sc for Mg Substitution. Journal of Superconductivity and Novel Magnetism, 2005, 18, 667-670.	0.5	2
72	The Material-Dependent Parameter Controlling the Universal Phase Diagram of Cuprates. Journal of Superconductivity and Novel Magnetism, 2005, 18, 773-777.	0.5	2

MICHELA FRATINI

#	Article	IF	CITATIONS
73	3D map of theranostic nanoparticles distribution in mice brain and liver by means of X-ray Phase Contrast Tomography. Journal of Instrumentation, 2018, 13, C01049-C01049.	1.2	2
74	Possible clean superconductivity in doped nanotube crystals. Journal of Physics and Chemistry of Solids, 2006, 67, 2187-2191.	4.0	1
75	Repeatability and reproducibility of intracellular molar concentration assessed by synchrotron-based x-ray fluorescence microscopy. AIP Conference Proceedings, 2016, , .	0.4	1
76	Combined use of X-ray fluorescence microscopy, phase contrast imaging for high resolution quantitative iron mapping in inflamed cells. Journal of Physics: Conference Series, 2017, 849, 012008.	0.4	1
77	The Challenge of the Vascularization of Regenerated Tissues. Fundamental Biomedical Technologies, 2018, , 139-149.	0.2	1
78	Numerical simulation of the blood oxygenation level–dependent functional magnetic resonance signal using finite element method. International Journal for Numerical Methods in Biomedical Engineering, 2020, 36, e3290.	2.1	1
79	Carbon-Nanotubes Field Emitter to be Used in Advanced X-ray Source. , 2014, , 358-365.		1
80	Hybrid Nanoparticles as Theranostics Platforms for Glioblastoma Treatment: Phototherapeutic and X-ray Phase Contrast Tomography Investigations. Journal of Nanotheranostics, 2022, 3, 1-17.	3.1	1
81	Combined X-ray Microfluorescence and Atomic Force Microscopy Studies of Mg Distribution in Whole Cells. , 2011, , .		0
82	Magnesium intracellular content and distribution map in drug-resistant and -sensitive whole cells. Journal of Biological Research (Italy), 2014, 87, .	0.1	0
83	Investigation of Herculaneum Papyri by X-Ray Phase-Contrast Tomography. , 2019, , 299-324.		0
84	Discovery of Lebambromyia in Myanmar Cretaceous Amber: Phylogenetic and Biogeographic Implications (Insecta, Diptera, Phoroidea). Insects, 2021, 12, 354.	2.2	0
85	Theoretical Analysis and Experimental Applications of X-ray Waveguides. , 2014, , 65-84.		0
86	3D imaging of theranostic nanoparticles in mice organs by means of x-ray phase contrast tomography. , 2018, , .		0